Near-Hover Control of a Helicopter with a Hanging Load

Narendra K. Gupta*
Systems Control, Inc., Palo Alto, Calif.

and

Arthur E. Bryson Jr.†
Stanford University, Stanford, Calif.

Piloting a helicopter with a hanging load is a difficult task, especially when the mass of the load is a significant fraction of the mass of the vehicle and there are gusty winds. An autopilot logic is proposed here for controlling the helicopter in this configuration and for precision hover. It is proposed that the vehicle position be measured using a lightweight cable from the helicopter to a point on the ground near the desired hover point. Simulation with one version of S-61 Sikorsky helicopter, shows satisfactory controller performance under both design conditions and for parameter changes from one mission to another. Assuming noise-free measurements for feedback is found to be far too optimistic in predicting performance, the sensor/estimator design is a key element in the controller.

I. Introduction

HELICOPTERS may be used more frequently in the future to transport heavy, bulky loads over short distances where surface transport is either infeasible or uneconomical, e.g., in off-loading containers from ships where port facilities are not available or carrying transmission towers or prefabricated buildings to remote sites. In many cases the load is transported hanging from cables fastened to the aircraft. Some reasons for this are: a) the load is too big to fit inside the aircraft; b) to save loading and unloading time; or c) the load is dangerous.

The pendulum motions of the hanging load couple into the motions of the helicopter to form an unstable system.[4,5,11,13] The instability is not severe and an experienced pilot can still control the helicopter.[3,14] However, the pilot workload is so great that the additional task of holding position (precision hover) is quite difficult, even in still air. On the other hand, an automatic control system can stabilize the system and perform additional tasks such as precision-hover even in strong gusty winds.[10,15-17]

To simplify the autopilot design and implementation, the complete system is modeled by four sub-systems which are approximately uncoupled.[6,12] These sub-systems are: a) a second-order system for yawing motion; b) a second-order system for vertical motion; c) a sixth-order system for longitudinal motion; and d) a sixth-order system for lateral motion. Controllers for only the sixth-order systems are designed here.

The vehicle position is determined using a lightweight measurement cable. Kalman filters are designed to estimate the state variables from three sensors: i) measurement cable angles; ii) load cable angles, and iii) fuselage attitude angles. The estimated states are used for feedback in the autopilot. A particular version of the Sikorsky S-61 is taken as the example helicopter.

For this system, changes in parameters are expected during a mission. In addition, some parameters are not known accurately in advance of the mission. The effect of the parameters on system behavior is studied using a fixed set of filter and controller gains.

Received Sept. 16, 1974; revision received May 9, 1975. This work was performed at Stanford University with financial support from U. S. Army Air Mobility, Ames Directorate, Ames, Calif. under contract NAS2-5143.

Index category: VTOL Handling, Stability, and Control.

*Senior Research Engineer. Member AIAA.

†Professor and Chairman of Aeronautics and Astronautics. Fellow AIAA.

Section II develops the equations of motion for the system and describes the measuring technique near hover. Section III describes the position and angle sensors. Section IV gives the design of the controller and the Kalman filter. The performance is studied under design and off-design conditions. The summary and conclusions are given in Sec. V.

II. Equations of Motion

A helicopter carrying a hanging load can be modeled as a system of three connected rigid bodies: a) rotor; b) fuselage; and c) hanging load. Since the rotor can be tilted much faster than the fuselage or the handling load, it suffices to use a quasi-steady rotor model. In this model it is assumed that the inclination of the rotor no-feathering plane (NFP) to the fuselage can be changed "instantaneously" using the cyclic pitch control. The hanging load is modeled as a rigid body pivoted about the suspension point at the fuselage. thus the dynamical system is simplified to two rigid bodies (the vehicle and the hanging load) connected at a pivot point.

This mathematical model is of 16th-order with four control variables. The state variables are: a) three position and three translational velocity coordinates of the vehicle center of mass; b) three angular orientation and three angular velocity coordinates of the fuselage; and c) two angular orientation and two angular velocity coordinates of the load cable. The control variables are the longitudinal and lateral inclinations of the rotor NFP relative to the fuselage, the collective pitch, and the tail rotor pitch. However, near hover, the yaw motion and the vertical motion are very nearly uncoupled from the longitudinal and the lateral motions. This results in a second-order model for yaw motion with tail rotor pitch as control, a second-order model for vertical motion with main rotor collective pitch as control, and a twelfth order model for longitudinal and lateral motions with longitudinal and lateral cyclic pitch as controls.

Figure 1 shows the coordinate system used to describe the motions of a helicopter carrying a hanging load. It is assumed that the load is carried by several cables attached to the helocopter at a point below its center of mass. The hanging load acts like a pendulum.

Let:

x,y,h	= longitudinal, lateral, and vertical position deviations from the desired hover point
u,v,w	= three components of linear velocity
φ,θ,ψ	= roll, pitch, and yaw angles
p,q,r	= roll, pitch, and yaw rates
R,v,ℓ	= subscripts for rotor, vehicle, and hanging load (or cable) respectively

$V_{w_x}, V_{w_y}, V_{w_z}$ = three components of wind velocity
I_x, I_y, I_z = vehicle moments of inertia about x,y and z axes
m_v = mass of vehicle
$\alpha_{(\cdot)}, \sigma_{(\cdot)}$ = drag coefficients
T = rotor thrust

The kinetic energy of the system is

$$T = \tfrac{1}{2}m_v[\dot{x}_v^2+\dot{y}_v^2+\dot{h}_v^2] + \tfrac{1}{2}m_\ell[\dot{x}_\ell^2+\dot{y}_\ell^2+\dot{h}_\ell^2] + \tfrac{1}{2}[I_x\dot{\varphi}_v^2+I_y\dot{\theta}_v^2+I_z\dot{\psi}_v^2] \quad (1)$$

and the potential energy is

$$V = m_v g h_v + m_\ell g h_\ell \quad (2)$$

which for small angles becomes

$$V = (m_v+m_\ell)gh_v - m_\ell g(b+\ell) + \frac{m_\ell g}{2}\left[b(\theta_v^2+\varphi_v^2)+\ell\left\{\left(\frac{x_\ell-x_v-b\theta_v}{\ell}\right)^2 + \left(\frac{-y_\ell+y_v-b\varphi_v}{\ell}\right)^2\right\}\right] \quad (3)$$

The equations of motion can be written using the Generalized Lagrange Method. The independent variables are h_v, ψ_v, θ_v, x_v, x_ℓ and φ_v, y_v, y_ℓ. In our model, the vertical motion (h_v and $\dot{h}_v$), and the yaw motion (ψ and $\dot{\psi}$) are uncoupled from the longitudinal-lateral motions. Since autopilot logic for these second-order subsystems is quite simple to design using collective pitch and tail-rotor pitch as controls, we shall henceforth consider only the longitudinal-lateral motions.

The equations governing θ_v, x_v, and x_ℓ (longitudinal motion) are

$$I_y\ddot{\theta}_v + m_\ell g b\theta_v + \frac{m_\ell g}{\ell}(x_\ell-x_v-b\theta_v)(-b) = Ta\theta_R - \alpha_1 I_y\dot{\theta}_v + \sigma_1 I_y(\dot{x}_v-V_{w_x}) + \alpha_3 I_y\dot{\phi}_v + \sigma_3 I_y(\dot{y}_v-V_{w_y}) + D_1\theta_R + D_2\phi_R \quad (4)$$

$$m_v\ddot{x}_v + \frac{m_\ell g}{\ell}(x_\ell-x_v-b\theta_v)(-1) = -T(\theta_v+\theta_R) + \alpha_2 m_v\dot{\theta}_v - \sigma_2 m_v(\dot{x}_v-V_{w_x}) - \alpha_4 m_v\dot{\phi}_v - \sigma_4 m_v(\dot{y}_v-V_{w_y}) - D_3\theta_R - D_4\phi_R \quad (5)$$

$$m_\ell\ddot{x}_\ell + \frac{m_\ell g}{\ell}[x_\ell-x_v-b\theta_v] = -m_\ell\sigma_5(\dot{x}_\ell-V_{w_x}) \quad (6)$$

The first term in the generalized force expressions on the right-hand side of Eqs. (4) and (5) is due to rotor cyclic pitch control, the next four terms represent damping and the last two terms arise from blade coning, offset distance of flapping hinge, and other effects. Expressions for D_1, D_2, D_3, and D_4 have been derived by Hall.[7] The only term on the right-hand side of Eq. (6) is due to air drag on the hanging load.

For small changes we can approximate T by the steady-state rotor thrust in the equations above to get

$$\ddot{\theta}_v + \frac{(\gamma-1)m_v gb}{I_y}\left[\frac{(b+\ell)}{\ell}\theta_v + \frac{x_v}{\ell} - \frac{x_\ell}{\ell}\right] = \frac{\gamma m_v ga + D_1}{I_y}\theta_R + \frac{D_2}{I_y}\phi_R - \alpha_1\theta_v + \sigma_1(\dot{x}_v-V_{w_x}) + \alpha_3\dot{\phi}_v + \sigma_3(\dot{y}_v-V_{w_y}) \quad (7a)$$

$$\ddot{x}_v + \{(\gamma-1)\frac{b}{\ell}+\gamma\}g\theta_v + \frac{(\gamma-1)g}{\ell}x_v - \frac{(\gamma-1)g}{\ell}x_\ell = \left(-\gamma g - \frac{D_3}{m_v}\right)\theta_R - \frac{D_4}{m_v}\phi_R + \alpha_2\dot{\theta}_v - \sigma_2(\dot{x}_v-V_{w_x}) - \alpha_4\dot{\phi}_v - \sigma_4(\dot{y}_v-V_{w_y}) \quad (7b)$$

$$\ddot{x}_\ell - \frac{b}{\ell}g\theta_v - \frac{g}{\ell}x_v + \frac{g}{\ell}x_\ell = -(\gamma-1)\sigma_5(\dot{x}_\ell-V_{w_x}) \quad (7c)$$

The equations for ϕ_v, y_v, and y_ℓ (lateral motion) can be written in a similar manner

$$\ddot{\phi}_v + \frac{(\gamma-1)m_v gb}{I_x}\left[\frac{(b+\ell)}{\ell}\phi_v - \frac{y_v}{\ell} + \frac{y_\ell}{\ell}\right] = \frac{\gamma m_v ga + D_1}{I_x}\phi_R - \frac{D_2}{I_x}\theta_R - \alpha_1'\phi_v - \sigma_1'(\dot{y}_v-V_{w_y}) - \alpha_3'\dot{\theta}_v + \sigma_3'(\dot{x}_v-V_{w_x}) \quad (8a)$$

$$\ddot{y}_v - \{(\gamma-1)\frac{b}{\ell}+\gamma\}g\phi_v + \frac{(\gamma-1)g}{\ell}y_v - \frac{(\gamma-1)g}{\ell}y_\ell = \left(\gamma g + \frac{D_3}{m_v}\right)\phi_R - \frac{D_4}{m_v}\theta_R - \alpha_2\dot{\phi}_v - \sigma_2(\dot{y}_v-V_{w_y}) - \alpha_4\dot{\theta}_v + \sigma_4(\dot{x}_v-V_{w_x}) \quad (8b)$$

$$\ddot{y}_\ell + \frac{b}{\ell}g\phi_v - \frac{g}{\ell}y_v + \frac{g}{\ell}y_\ell = -(\gamma-1)\sigma_5(\dot{y}_\ell-V_{w_y}) \quad (8c)$$

The longitudinal and lateral motions are coupled by cross damping forces and torques and by cross controls. However, the controls can be approximately uncoupled by taking linear combinations of θ_R and ϕ_R as new controls. If this is done, the approximation of longitudinal-lateral decoupling is good for designing controllers and filters.

A particular version of the Sikorsky S-61 is the example helicopter.[8] It weighs 6000 kg and carries 2000 kg hanging load on a 20 m-long cable, attached to a point 1.5 m below its center of mass. The state dynamics matrix and the control and noise distribution matrices are given in Table 1 for the coupled longitudinal-lateral motions of this system. Values of stability derivatives for this vehicle are taken from Hall and

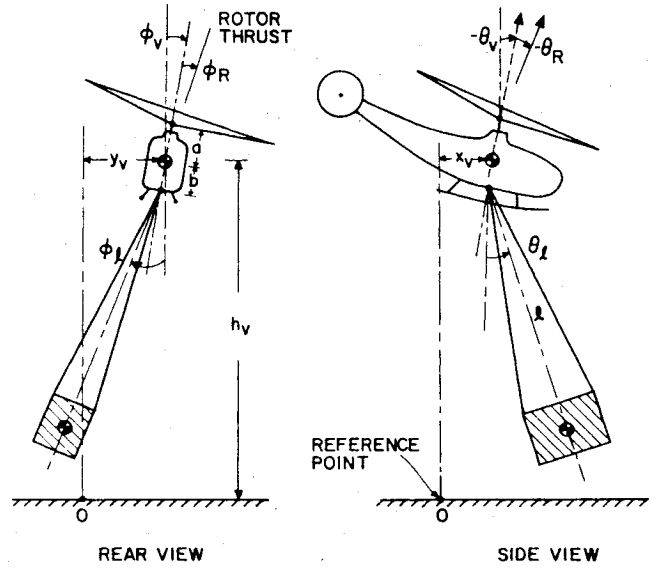

Fig. 1 Helicopter carrying a hanging load.

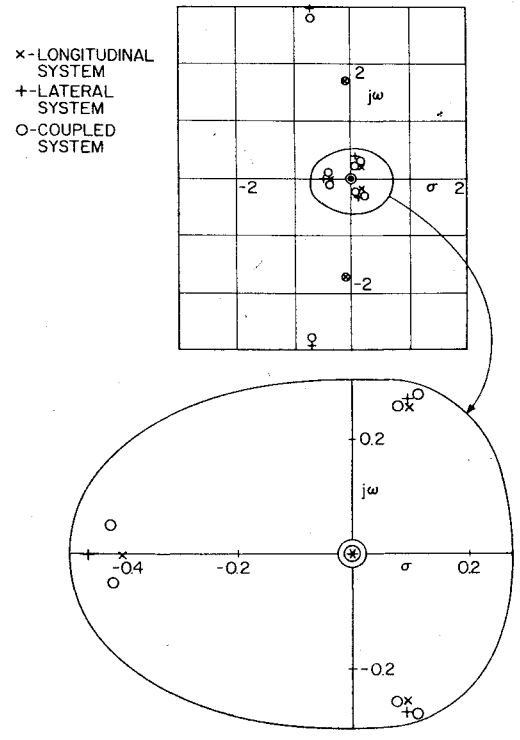

Fig. 2 Poles of the open-loop systems.

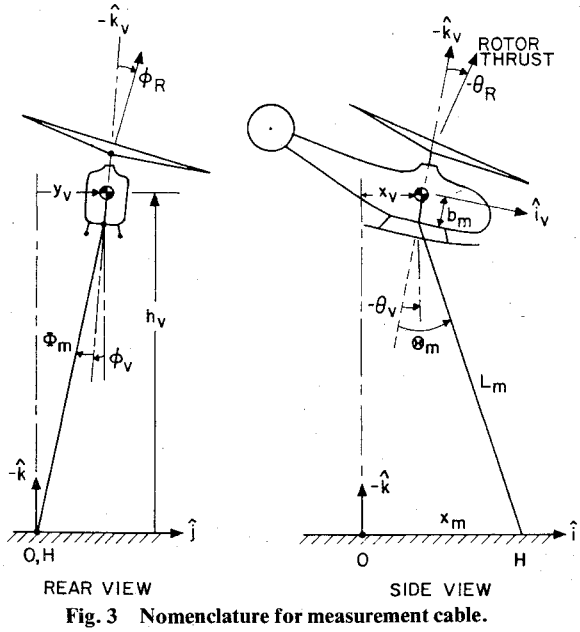

Fig. 3 Nomenclature for measurement cable.

Bryson.[9] The drag coefficient on the hanging load is based on the secant slope between zero and 7.0 m sec^{-1} velocity. The portion of the state distribution matrix inside broken lines represents dynamic coupling between the longitudinal and lateral motions.

The control vector is redefined so that its two components are linear combinations of θ_R and φ_R. If $u^T \triangleq (\theta_R + .03\varphi_R, \varphi_R - .03\theta_R)$ the modified control distribution matrix G is shown in Table 1, so that cross-control enters only into the vehicle moments and not into vehicle forces.

The decoupling approximation is made. The control u_1 affects the longitudinal motion and u_2 the lateral motion. The state definition matrices for the longitudinal and the lateral system are the appropriate portions of the matrices in Table 1. Figure 2 shows the eigenvalues of the uncontrolled longitudinal and lateral systems. Also shown are the corresponding eigenvalues of the coupled twelfth-order system. The eigenvalues for the coupled and the decoupled system are very near to each other showing that the decoupling approximation is reasonable.

III. Position and Angle Sensors

To do an adequate control job it is necessary to sense fuselage angles, load cable angles, and fuselage position relative to a desired hover point.§

The position sensor suggested here consists of a second cable (a lightweight "measurement cable") fastened to a point on the ground, which passes through a ring mounted elastically in the plane of the aircraft floor, and is held by a constant tension winch inside the aircraft (Figs. 3 and 4). The portion of the cable above the aircraft floor is parallel to a reference axis fixed to the aircraft.¶ The forces in the springs are measured using strain gages, while a potentiometer in the constant tension wnich measures the length of the cable. Let θ_m and ϕ_m be the inclinations of the cable to the aircraft reference axis and ℓ_m the length of the cable when the aircraft is hovering at reference position with reference orientation. In a perturbed position the deviations $\delta\theta_m$, $\delta\phi_m$ and $\delta\ell_m$ from reference values are given as[18]

$$\delta\ell_m \cong \sec\theta_m \delta h_v + \ell_m \tan\theta_m \theta_v \tag{9}$$

$$\delta\phi_m \cong \frac{\sec\theta_m}{\ell_m} y_v - \left(1 + \frac{b_m}{\ell_m}\sec\theta_m\right)\phi_v + \tan\theta_m \psi_v \tag{10}$$

$$\delta\theta_m \cong \sec\theta_m\left(\sec\theta_m + \frac{b_m}{\ell_m}\right)\theta_v - \frac{\sec\theta_m}{\ell_m} x_v + \tan\theta_m \delta h_v \tag{11}$$

The angles between the cable carrying the hanging load and the fuselage reference axis could be measured in the same way using another elastically mounted ring. Thus

$$\theta_{\ell v} = \theta_\ell - \theta_v = -\theta_v\left(1 + \frac{b}{\ell}\right) - \frac{x_v}{\ell} + \frac{x_\ell}{\ell}$$

$$\phi_{\ell v} = \phi_\ell - \phi_v = -\phi_v\left(1 + \frac{b}{\ell}\right) + \frac{y_v}{\ell} - \frac{y_\ell}{\ell} \tag{12}$$

The fuselage attitude θ_v and ϕ_v could be obtained using an onboard Inertial Measurement Unit (IMU) or a vertical gyro.

All these measurements contain errors which we model as additive white noise. The measurement vector z for the two systems can be written as

$$z = Hx + v \tag{13}$$

where

$$E[\theta(t)\theta^T(\tau)] = R\,\delta(t-\tau) \tag{14}$$

For the example helicopter, we have taken the measurement cable to be 35 m long, offset 25 m in the longitudinal direction from the desired hover point on the ground. Table 2 gives the nonzero elements of the matrices H and R used in the example design.

IV. Design and Performance of a Precision Hover Autopilot

The control logic for precision hover is designed using quadratic synthesis. Since the correlation time of the wind velocity changes is comparable to or greater than the time

§The system is observable without the fuselage angles but the resulting estimate error variances are far too large to be acceptable.

¶In practice the measurement cable could *not* be fastened below the mass center of the fuselage. This would make the relations (9-11) more complicated, but would not change the principle.

Table 1 State definition matrices for one version of Sikorsky S-61 carrying a 2000 kg hanging load[a]

	F												G_u		Γ		G	
θ_v	0.0	1.0	0.0	0.0	0.0	0.0	0.0	0.0	0.0	0.0	0.0	0.0	0.0	0.0	0.0	0.0	0.0	0.0
$\dot{\theta}_v$	−2.25	−.415	−.104	.0111	.104	0.0	0.0	.318	0.0	.00381	0.0	0.0	8.38	.393	−.0111	−.00381	8.38	.139
x_v	0.0	0.0	0.0	1.0	0.0	0.0	0.0	0.0	0.0	0.0	0.0	0.0	0.0	0.0	0.0	0.0	0.0	0.0
$\dot{x}_v$	−13.3	1.43	−.164	−.0198	.164	0.0	0.0	−.311	0.0	−.0059	0.0	0.0	−13.1	−.396	.0198	.0059	−13.1	0.0
x_ℓ	0.0	0.0	0.0	0.0	0.0	1.0	0.0	0.0	0.0	0.0	0.0	0.0	0.0	0.0	0.0	0.0	0.0	0.0
$\dot{x}_\ell$	.736	0.0	.491	0.0	−.491	−.0026	0.0	0.0	0.0	0.0	0.0	0.0	0.0	0.0	.0026	0.0	0.0	0.0
ϕ_v	0.0	0.0	0.0	0.0	0.0	0.0	0.0	1.0	0.0	0.0	0.0	0.0	0.0	0.0	0.0	0.0	0.0	0.0
$\dot{\phi}_v$	0.0	−1.23	0.0	.0136	0.0	0.0	−8.28	−1.58	.385	−.0407	−.385	0.0	−1.43	30.7	−.0136	.0407	−.465	30.8
y_v	0.0	0.0	0.0	0.0	0.0	0.0	0.0	0.0	0.0	1.0	0.0	0.0	0.0	0.0	0.0	0.0	0.0	0.0
$\dot{y}_v$	0.0	−.311	0.0	.0059	0.0	0.0	13.3	−1.43	−.164	−.0198	.164	0.0	−.396	13.1	−.0059	.0198	0.0	13.1
y_ℓ	0.0	0.0	0.0	0.0	0.0	0.0	0.0	0.0	0.0	0.0	0.0	1.0	0.0	0.0	0.0	0.0	0.0	0.0
$\dot{y}_\ell$	0.0	0.0	0.0	0.0	0.0	0.0	−.736	0.0	.491	0.0	−.491	−.0026	0.0	0.0	0.0	.0026	0.0	0.0
	$[\theta_v$	$\dot{\theta}_v$	x_v	$\dot{x}_v$	x_ℓ	$\dot{x}_\ell$	ϕ_v	$\dot{\phi}_v$	y_v	$\dot{y}_v$	y_ℓ	$\dot{y}_\ell]$	$[\theta_R$	$\phi_R]$	$[V_{w_x}$	$V_{w_y}]$	$[\theta_R+.03\phi_R,\ \phi_R-.03\theta_R]$	
					x^T								u_0^T		w		u^T	

[a] Units in meters, secs, radians.

Table 2 Nonzero elements of matrices H and R

Measurement definition matrices for the longitudinal system

x	H^T:		
θ_v	−1.537	−1.075	1.0
x_v	−.0348	−.05	0.0
x_ℓ	0.0	.05	0.0
	$z=[\delta\theta_m$	$\theta_{\ell v}$	$\theta_v]$

Noise covariance matrix

$R=\text{diag}\,[6\times10^{-5}\quad 6\times10^{-5}\quad 1.5\times10^{-5}]$

Measurement definition matrices for the lateral system

x	H^T:		
ϕ_v	−1.052	−1.075	1.0
y_v	.0348	.05	0.0
y_ℓ	0.0	−.05	0.0
	$z=[\delta\phi_m$	$\phi_{\ell v}$	$\phi_v]$

Noise covariance matrix

$R=\text{diag}\,[6\times10^{-5}\quad 6\times10^{-5}\quad 1.5\times10^{-5}]$

Table 3 Feedback gains for longitudinal and lateral systems

Controller performance indices

$$J_{\text{longitudinal}}=E\left\{\left(\frac{\theta_v}{.2}\right)^2+\left(\frac{x_v}{2}\right)^2+\left(\frac{x_\ell}{1.0}\right)^2+\left(\frac{u_1}{.1}\right)^2\right\}_{s.s}$$

$$J_{\text{lateral}}=E\left\{\left(\frac{\phi_v}{.2}\right)^2+\left(\frac{y_v}{2}\right)^2+\left(\frac{y_\ell}{1.0}\right)^2+\left(\frac{u_2}{.1}\right)^2\right\}_{s.s}$$

State feedback gains (units m, sec, rad)

c_{θ_v}	$c_{\dot{\theta}_v}$	c_{x_v}	$c_{\dot{x}_v}$	c_{x_ℓ}	$c_{\dot{x}_\ell}$	c_{w_x}
−1.27	−.277	.141	.157	−.0296	.137	.00239

c_{ϕ_v}	$c_{\dot{\phi}_v}$	c_{y_v}	$c_{\dot{y}_v}$	c_{y_ℓ}	$c_{\dot{y}_\ell}$	c_{w_ℓ}
−.834	−.125	−.137	−.131	.0249	−.141	−.00228

Closed loop eigenvalues of coupled and decoupled systems

7th-order longitudinal system [sec^{-1}]	7th-order lateral system [sec^{-1}]	Complete 14th-order system [sec^{-1}]
$-.99\pm1.8j$		$-.93\pm1.9j$
$-.58\pm1.0j$		$-.57\pm1.1j$
$-.84\pm.78j$		$-.91\pm.62j$
	$-2.2\pm3.5j$	$-2.3\pm3.5j$
	$-.82\pm.74j$	$-.72\pm.79j$
	$-.53\pm1.0j$	$-.50\pm.98j$
−.2	−.2	−.2, −.2 (double root)

constants associated with the system, the wind velocity is modeled as a first-order Markov process with a 5 sec time constant.

$$\dot{V}_{w_x}=-\frac{1}{\tau_c}V_{w_x}+\eta_x \qquad \tau_c=5\ \text{sec} \tag{15}$$

where η_x is white noise. If the RMS value of V_{w_x} is taken as 7 m sec^{-1}, the required spectral density of η_x is

$$Q_{\eta_x}=\frac{2\times7^2}{5}=19.6\ m^2\ \text{sec}^{-3} \tag{16}$$

There is, of course, a similar equation for the lateral wind disturbance.

If Eq. (15) is adjoined to the longitudinal equations, the system is modified to

$$\frac{\mathrm{d}}{\mathrm{d}t}\left[\begin{array}{c}x\\\hline V_{w_x}\end{array}\right]=\left[\begin{array}{c|c}F & \Gamma\\\hline 0 & -1/\tau_c\end{array}\right]\left[\begin{array}{c}x\\\hline V_{w_x}\end{array}\right]+\left[\begin{array}{c}G\\\hline 0\end{array}\right]u+\left[\begin{array}{c}0\\\hline 1\end{array}\right]\eta_x \tag{17}$$

where x, u, F, Γ, and G are defined in Table 1. We choose a control law such that u is a linear combination of x and V_{w_x}, i.e.

$$u=Cx+c_{w_x}V_{w_x} \tag{18}$$

u is a scalar in this case; hence, C is a row vector and c_{w_x} is a scalar. Substituting for u in Eq. (17)

$$\frac{\mathrm{d}}{\mathrm{d}t}\left[\begin{array}{c}x\\\hline V_{w_x}\end{array}\right]=\left[\begin{array}{c|c}F+GC & \Gamma+Gc_{w_x}\\\hline 0 & -1/\tau_c\end{array}\right]\left[\begin{array}{c}x\\\hline V_{w_x}\end{array}\right]+\left[\begin{array}{c}0\\\hline 1\end{array}\right]\eta_x \tag{18}$$

Notice that the closed loop eigenvalues depend on state definition matrices and the gains C and do not depend on gain c_{w_x}. Hence we can choose gains C and c_{w_x} independently; C to obtain the desired dynamics of the closed loop system, and c_{w_x} to achieve good performance in the presence of wind.

In the design procedure adopted here, the gains C are chosen using the quadratic synthesis procedure, i.e., by minimizing a performance index, J which is quadratic in state and control variables. The gain c_{w_x} can be chosen to minimize the steady state rms value of a desired linear combination of state variables (in this case the error in position of the hanging load). Thus, the effect of wind can be minimized without making the closed loop system too "fast."[18]

The feedback gains on the state variables and wind velocity were computed using the OPTSYS computer program of Hall,[7] and are shown in Table 3 for the longitudinal and lateral systems. The closed loop eigenvalues of the decoupled longitudinal and lateral systems are compared with the closed loop eigenvalues of the coupled longitudinal-lateral system (using gains from the decoupled systems) in Table 3. The

Table 4 System rms response in 7 m sec^{-1} rms longitudinal and lateral wind[a]

Longitudinal system							
	θ_v	$\dot{\theta}_v$	x_v	$\dot{x}_v$	x_ℓ	$\dot{x}_\ell$	$u_1 (\approx \theta_R)$
Perfect state information	.00331	.00601	.0383	.0297	.0223	.0183	.00948
Noisy measurements and filter	.0341	.0737	.404	.313	.470	.241	.0247
Lateral system							
	ϕ_v	$\dot{\phi}_v$	y_v	$\dot{y}_v$	y_ℓ	$\dot{y}_\ell$	$u_2 (\approx \phi_R)$
Perfect state information	.00338	.00873	.0391	.0299	.0183	.0153	.00939
Noisy measurements and filter	.0328	.102	.339	.287	.393	.202	.0183

[a] All in units of m, sec, rad.

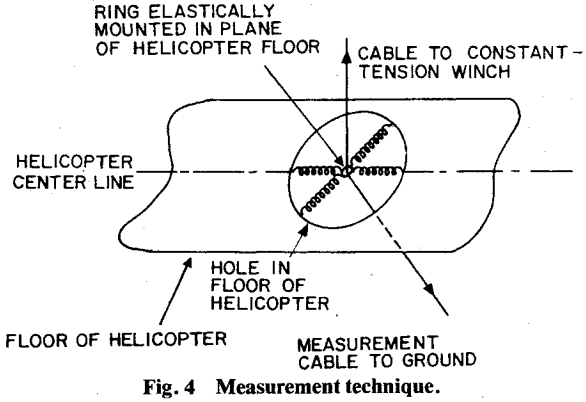

Fig. 4 Measurement technique.

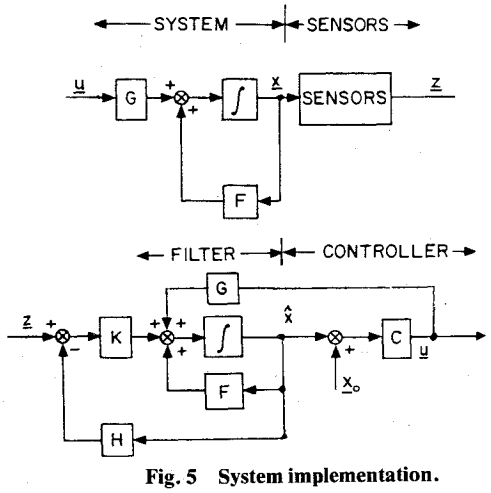

Fig. 5 System implementation.

eigenvalues are quite close showing again that the decoupling approximation is reasonable. Notice, also, that each mode has adequate damping.

The root-mean-square (rms) response of the system is determined assuming perfect state information (Ref. 1, Chap. 15). Table 4 first row, shows the rms values of the state and control variables. The rms errors are quite small.

A filter is designed to estimate the state variables and the wind velocity from the noisy measurements. If $\hat{x}$ is the estimated value of x, then the estimation equation for the longitudinal system is

$$\frac{\mathrm{d}}{\mathrm{d}t}\begin{bmatrix}\hat{x}\\ \hat{V}_{w_x}\end{bmatrix}=\left[\begin{array}{c|c} F & \Gamma \\ \hline 0 & -1/\tau_c \end{array}\right]\begin{bmatrix}\hat{x}\\ \hat{V}_{w_x}\end{bmatrix}+\begin{bmatrix}G\\ 0\end{bmatrix} \times u+K(z-H\hat{x}) \qquad (19)$$

Table 5 Filters for longitudinal and lateral system[a]

	$K_{\text{longitudinal}}$				K_{lateral}		
x				x			
θ_v	−.661	−.482	2.51	ϕ_v	−.670	−.733	3.37
$\dot{\theta}_v$	−.161	−1.07	4.49	$\dot{\phi}_v$	−1.94	−1.92	7.65
x_v	−17.8	−.494	−35.0	y_v	18.6	1.42	25.0
$\dot{x}_v$	−.626	2.60	−26.7	$\dot{y}_v$	3.08	−1.66	21.6
x_ℓ	−16.9	3.58	−19.5	y_ℓ	16.6	−3.68	11.1
$\dot{x}_\ell$	−5.13	−.142	−9.25	$\dot{y}_\ell$	5.47	.544	6.12
V_{w_x}	257	203	−717	V_{w_y}	−204	−245	796
$z^T = [\theta_m$		θ_{ℓ_v}	$\theta_v]$	$z^T = [\phi_m$		ϕ_{ℓ_v}	$\phi_v]$

[a] All in units of m, sec, rad.

where z and H were defined for the longitudinal and lateral systems before. The 7×3 gain matrix K is given in Table 5. The rms response of the system is determined with the filter and the controller designed above in the presence of 7 m sec^{-1} rms longitudinal and lateral wind and is compared to the perfect measurements case in Table 4. There is a considerable increase in rms deviation of the hanging load position and control as compared to the case with perfect state information. Nevertheless, the errors are small for such a strong gusty wind.

Figure 5 shows how the system can be implemented. The complete system is divided into four parts: a) controller; b) system dynamics; c) sensors; and d) filter.

It is possible to eliminate steady errors in postion of the hanging load caused by steady winds by the use of integral control. The new states which are integrals of the longitudinal and lateral errors in position of the hanging load are used for feedback. The technique is demonstrated in Ref. 18.

Performance Under Off-Design Conditions

In operation some of the parameters will differ from the values used in designing the control system, e.g., in off-loading container ships, all containers may not have the same mass (change in γ) or location of the center of mass (change in ℓ). In addition, the values of some of the system parameters may not be accurately known. Therefore the performance of the system was studied when the gains for the design condition are used with a different configuration.

We believe the following four parameters are the most likely ones to change in normal operation: a) mass of the vehicle, because of varying amounts of fuel; b) mass of the hanging load (or the ratio $\gamma=(m_v+m_\ell)/m_v$; c) the distance between the suspension point and the center of gravity of the hanging load; d) drag coefficient on the hanging load.

These parameters are changed one at a time and rms state response is determined (see Table 6) using controller and filter gains from design conditions. The rms error in position of the

Table 6 RMS response with noisy measurements and filter[a] (off-design conditions)

				rms state and control						
m_v	$\gamma=m_v+m_\ell/m_v$	ℓ	$(\gamma-1)\sigma_5$[b]	θ_v	$\dot{\theta}_v$	x_v	$\dot{x}_v$	x_ℓ	$\dot{x}_\ell$	$u_1(\approx\theta_R)$
6000	1.33	20	.0026	.0341	.0737	.404	.313	.470	.241	.0247[c]
6000	1.33	10	.0026	.0244	.0599	.369	.259	.465	.217	.0234
6000	1.33	30	.0026	.0400	.0808	.428	.342	.484	.257	.0258
5000	1.33	20	.0026	.0368	.0788	.409	.330	.472	.244	.0260
7000	1.33	20	.0026	.0323	.0702	.400	.301	.469	.239	.0240
6000	1.5	20	.0026	.0273	.0671	.395	.277	.474	.224	.0226
6000	1.167	20	.0026	.0515	.0892	.467	.427	.494	.312	.0283
6000	1.33	20	.00026	.0508	.0883	.464	.422	.491	.307	.0282
6000	1.33	20	.026	.0593	.100	.561	.507	.770	.405	.0289

[a]Units in kg, m, sec; angles in rad. [b]Drag coefficient on hanging load. [c]Design condition.

hanging load does not deteriorate very much except with increased drag on the hanging load. Since a satisfactory system behavior is obtained by using fixed controller and filter gains, it seems unnecessary to change gains with nominal variations in system parameters.

V. Summary and Conclusions

A mathematical model is developed for the motions of a hovering or slowly moving helicopter carrying a hanging load. Autopilot logic is proposed for position-hold (hover) such that all helicopter-hanging load modes have adequate damping.

For the example helicopter it is shown that the longitudinal-lateral decoupling approximation is satisfactory for the purpose of hover autopilot design.

The root mean square (rms) response of the controlled system is quite satisfactory in the presence of gusty longitudinal and lateral winds. Further improvements in hovering accuracy could be attained by using a better measurement system, since substantially better performance is obtained using the assumption of perfect state information (ideal case) under design conditions.

The stability and performance of the system is examined for reasonable variations in system parameters. In no case does the system become unstable. The rms response does not change appreciably except with a tenfold increase in drag coefficient on the hanging load. The behavior is satisfactory in all studied cases.

References

[1]Bryson, A. E., Jr. and Ho, Y. C., *Applied Optimal Control*, Blaisdell, Waltham, Mass., 1969.

[2]Bryson, A. E. and Hall, W. E., Jr., "Optimal Control and Filter Synthesis by Eigenvector Decomposition," Stanford University Department of Aeronautics and Astronautics, Report No. 436, Nov. 1971.

[3]Dukes, T. A., "Maneuvering Heavy Sling Loads Near Hover," presented at the *28th National Forum of the American Helicopter Society*, Washington, D. C., Preprint No. 630, May 1972.

[4]Etkin, B. and Mackworth, J. C., "Aerodynamic Instability of Non-Lifting Bodies Towed Beneath an Aircraft," University of Toronto, Institute of Aerophysics, Technical Note No. 65, Jan. 1963.

[5]Gabel, R. and Wilson, G. J., "Test Approaches to External Sling Load Instabilities," *Journal of the American Helicopter Society*, Vol. 15, July 1968, pp. 44-55.

[6]Gessow, A. and Meyers, G. C., Jr., *Aerodynamics of the Helicopter*, McMillan, N.Y., 1952.

[7]Hall, W. E., Jr., "Computational Methods for the Synthesis of Rotary Wing VTOL Aircraft Control Systems," Ph.D. Dissertation, Department of Aeronautics and Astronautics, Stanford University, Aug. 1971.

[8]Hall, W. E., Jr. and Bryson, A. E., Jr., "The Inclusion of Rotor Dynamics in Controller Design for Helicopters," *Journal of Aircraft*, Vol. 10, April 1973, pp. 200-206.

[9]Hall, W. E., Jr. and Bryson, A. E., Jr., "Synthesis of Hover Autopilots for Rotary-Wing VTOL Aircraft," Stanford University, Department of Aeronautics and Astronautics, Report No. 446, June 1972.

[10]Keane, W. P. and Milelli, R. J., "IFR Hover for Heavy Lift Helicopters with Slung Load," presented at the *27th Annual National V/STOL Forum of the American Helicopter Society*, Washington, D. C., Preprint No. 540, May 1071.

[11]Lucassen, L. R. and Sterk, F. J., "Dynamic Stability Analysis of a Hovering Helicopter with a Slung Load," *Journal of the American Helicopter Society*, Vol. 10, April 1965, pp. 6-12.

[12]Nikolsky, A. A., *Helicopter Design*, Wiley, N.Y., 1951.

[13]Poli, C. and Cromack, D., "Dynamics of Slung Bodies Using a Single Point Suspension System," *Journal of Aircraft*, Vol. 10, Feb. 1973, pp. 80-86.

[14]Szustak, L. S. and Jenney, D. S., "Control of Large Crane Helicopters," *Journal of the American Helicopter Society*, Vol. 16, July 1971, pp. 11-22.

[15]Wolkovich, J. and Johnston, D. E., et al., "Automatic Control Considerations for Helicopters and VTOL Aircraft With and Without Sling Loads," TR 145-1, Systems Technology, Inc., Hawthorne, Calif., May 1966.

[17]Asseo, S. J. and Whitbeck, R. F., "Control Requirements for Sling-Load Stabilization in Heavy Lift Helicopters," *Journal of the American Helicopter Society*, Vol. 18, July 1973, pp. 23-31.

[18]Gupta, N. K. and Bryson, A. E., Jr., "Automatic Control of a Helicopter with a Hanging Load," Stanford University, Department of Aeronautics and Astronautics, Report No. 459, June 1973.